Chapter 16

The Use of an Adeno-Associated Viral Vector for Efficient Bicistronic Expression of Two Genes in the Central Nervous System

Thomas Haynes Hutson, Claudia Kathe, Sean Christopher Menezes, Marie-Claire Rooney, Hansruedi Bueler, and Lawrence David Falcon Moon

Abstract

Recombinant adeno-associated viral (AAV) vectors are one of the most promising therapeutic delivery systems for gene therapy to the central nervous system (CNS). Preclinical testing of novel gene therapies requires the careful design and production of AAV vectors and their successful application in a model of CNS injury. One major limitation of AAV vectors is their limited packaging capacity (<5 kb) making the co-expression of two genes (e.g., from two promoters) difficult. An internal ribosomal entry site has been used to express two genes: However, the second transgene is often expressed at lower levels than the first. In addition to this, achieving high levels of transduction in the CNS can be challenging. In this chapter we describe the cloning of a bicistronic AAV vector that uses the foot-and-mouth disease virus 2A sequence to efficiently express two genes from a single promoter. Bicistronic expression of a therapeutic gene and a reporter gene is desirable so that the axons from transduced neurons can be tracked and, after CNS injury, the amount of axonal sprouting or regeneration quantified. We go on to describe how to perform a pyramidotomy model of CNS injury and the injection of AAV vectors into the sensorimotor cortex to provide efficient transduction and bicistronic gene expression in cortical neurons such that transduced axons are detectable in the dorsal columns of the spinal cord.

Key words AAV, CNS injury, Regeneration-associated gene, Bicistronic vector, 2A sequence, Ribosomal skipping, Self-cleavage, Intracortical injection, Pyramidotomy

1 Introduction

Following an injury to the central nervous system (CNS) neurons undergo collateral sprouting but very limited long-distance regeneration which results in their failure to form functional connections with their original targets. This is due in part to the reduced intrinsic growth state of mature CNS neurons, which is characterized by their failure to express regeneration-associated genes (RAGs) after an injury [1–5]. Steady advancements in molecular neurobiology

Andrew J. Murray (ed.), *Axon Growth and Regeneration: Methods and Protocols*, Methods in Molecular Biology, vol. 1162,
DOI 10.1007/978-1-4939-0777-9_16,

have elevated gene therapy into a promising therapeutic strategy for increasing the expression of RAGs and improving regeneration after a CNS injury [6–9].

To test a potential gene therapy an in vivo model of CNS injury is required. The corticospinal tract (CST) is present in all mammals and originates from the pyramidal corticospinal neurons (CSNs) in layer V of the cerebral cortex that project axons through the brainstem to the spinal cord. The CST fibers descend through the ventral brainstem in the medullary pyramids after which the main component of the CST decussates at the spinomedullary junction to form the dorsal CST which runs in the ventral portion of the contralateral dorsal funiculus in the adult rat [10]. The CST is a descending motor pathway that primarily controls locomotion, posture, and voluntary skilled movements [11]. Following injury to the rodent CST, persistent deficits in sensorimotor function are observed and restorative strategies are often assessed using behavioural tests of sensorimotor and skilled motor function [11–14]. The CST can be lesioned by performing a unilateral pyramidotomy (i.e., one of the medullary pyramids is cut) [15]. This leads to the anterograde degeneration of the injured axons and functional deficits on the contralateral side of the body. These deficits can be overcome by enhancing the growth state of the uninjured CSNs, allowing them to sprout their axons across the midline and reinnervate the area denervated by the lesion. The pyramidotomy model has been extensively used to assess potential therapies to enhance neuronal regeneration and sprouting and functional recovery following CNS injury [8, 16]. However, efficient, widespread transduction of the CSNs in the cortex is challenging and has only been achieved when high titers (1×10^{14} genome copies (GC)/mL) and slow infusion rates were used [6, 8, 17]. Here we outline a procedure to inject AAV vectors into the cortex to transduce CSNs and then perform a pyramidotomy injury.

Recombinant adeno-associated viral (AAV) vectors represent one of the most attractive gene delivery systems for the CNS due to their ability to efficiently transduce neurons and to provide long-term expression with only a minimal immune response [18, 19]. AAV vectors have one of the best characterized safety profiles and have been taken to clinical trial for a number of neurodegenerative diseases [20, 21]. In addition to this, Glybera (an AAV vector encoding lipoprotein lipase) has recently been approved for use in the EU to reduce the incidence of pancreatitis in people with inherited lipoprotein lipase deficiency [22] and paves the way for further AAV-based gene therapies for other conditions. Each AAV serotype expresses different capsid proteins that determine which receptors the AAV vector can bind to for cell entry and therefore establishes the AAV vector's tropism [23]. Pseudotyping AAV2 genome with the capsid from different AAV serotypes can generate vectors with different tissue and cellular tropisms, which can improve the efficiency and pattern of transduction in specific

regions of the CNS [24–26]. We have previously shown that AAV1 is the optimal serotype for transducing CSNs in adult rats [17] although other AAVs also work well: AAV5 [27–29] and AAV8 [6, 28, 30]. Viral vector-mediated over-expression of pro-regenerative genes, including retinoic acid receptor, beta (RARbeta2), neuronal calcium sensor 1 (NCS1), and Kruppel-like factor 7 (KLF-7), have been shown to enhance the intrinsic growth state of CSNs and facilitate axonal regeneration after injury [6–9]. However, these studies have either used viral vectors with larger insert capacities such as lentiviral vectors or used two separate AAV vectors: one encoding a RAG and the other a reporter gene. It would therefore be very valuable to have an AAV vectors which can co-express a pro-regenerative gene together with a fluorescent reporter so that transduced axons can be distinguished from axons that are not transduced: this would increase our ability to identify useful pro-regenerative therapies.

A disadvantage of AAV vectors is their relatively low insert capacity which can be an issue if two genes are required to be expressed (e.g., from two promoters). One partial solution is to use a single promoter which drives two genes linked by an internal ribosomal entry site (IRES) [31, 32]: typically, the RAG would be expressed immediately downstream of the promoter, whilst the fluorescent reporter gene is expressed downstream of the IRES. Although this works reasonably well, the IRES-dependent second gene is usually expressed at a significantly lower level, estimated at tenfold less than the cap-dependent first gene [33, 34]. To date we know of no reports where transduction of supraspinal neuronal cell bodies with such an AAV vector results in detectable labelling of their axons in the spinal cord.

This problem can be mitigated by using the 2A peptide from the foot-and-mouth disease virus (FMDV) [35]. The 2A peptide sequence is only 24 amino acids long and can mediate efficient bicistronic expression of two gene products from a single promoter by undergoing ribosomal skipping (referred to as "self-cleavage") during protein translation. Theoretically, the two gene products are expressed in a 1:1 ratio, and in practice each gene product is expressed at a high level. The 2A and 2A-like bicistronic systems have been shown to be highly effective in the CNS where high expression levels of both genes have been demonstrated [6, 34].

2 Materials

2.1 Chemicals and Solutions

Plasmids: The psubCMV-2A-WPRE plasmid (Fig. 1a) was a kind gift from Dr. Hansruedi Bueler, University of Kentucky. The plasmid contains a *cytomegalovirus* (CMV) promoter (to drive expression of the bicistron), the FMDV 2A sequence, and a woodchuck hepatitis virus post-transcriptional regulatory element (WPRE). The 2A sequence is immediately flanked by an upstream (i.e., 5′)

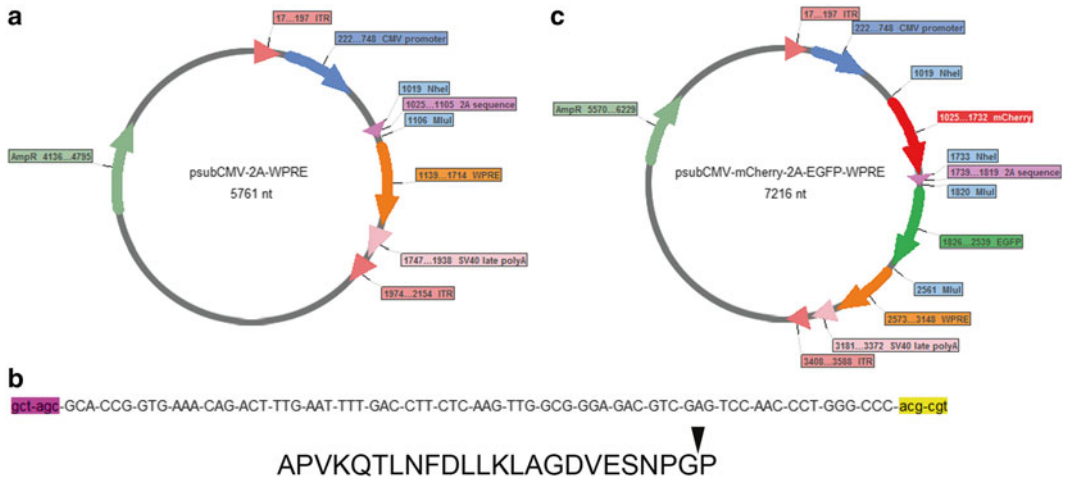

Fig. 1 (**a**) psubCMV-2A-WPRE plasmid map showing NheI site for cloning a transgene immediately downstream of the CMV promoter (and upstream of the 2A sequence) and an MluI site for cloning a transgene downstream of the 2A sequence. (**b**) Nucleotide sequence showing NheI restriction site (*lower case*, *pink*), the 2A sequence (*upper case*), and MluI restriction site (*lower case*, *yellow*). The 2A sequence encodes 24 amino acids APVKQTLNFDLLKLAGDVESNPGP, the *arrowhead* indicates the ribosome skipping ("self-cleavage") site. (**c**) psubCMV-mCherry-2A-EGFP-WPRE plasmid map showing mCherry cloned upstream and EGFP downstream of the 2A sequence

NheI restriction site and a downstream (i.e., 3′) MluI restriction site (Fig. 1b), *see* **Note 1**.

Enzymes: NheI and MluI, NEBuffer 4, and BSA (NEB, UK). Alkaline phosphatase (calf intestinal) (NEB, UK).

PCR reagents: Vent DNA polymerase (NEB, UK), 10× Vent DNA polymerase buffer, DMSO, 10 mM Nucleotide mix (Promega, UK), 100 mM $MgSO_4$, 100 μM forward and reverse primers, 50 ng plasmids containing mCherry or EGFP, PCR-grade nucleotide-free H_2O.

Anaesthetic: 0.5 mg/kg Domitor (medetomidine hydrochloride) and 100 mg/kg Vetalar (ketamine hydrochloride) or with a mixture of isoflurane (1.5 %) and O_2 (1 L/min).

Analgesia: 5 mg/kg Carprofen was administered subcutaneously for postoperative analgesia.

Euthanasia solutions: 400 mg/kg Lethabarb (sodium pentobarbital).

2.2 Cloning Strategy and Primer Design

Our goal was to generate a series of plasmids with the generic structure (AAV-RAG-2A-EGFP). First, we cloned EGFP downstream of 2A, and then we cloned mCherry upstream of 2A. The resulting plasmid (AAV-mCherry-2A-EGFP-WPRE) (Fig. 1c) has been used in many of our experiments as a negative control

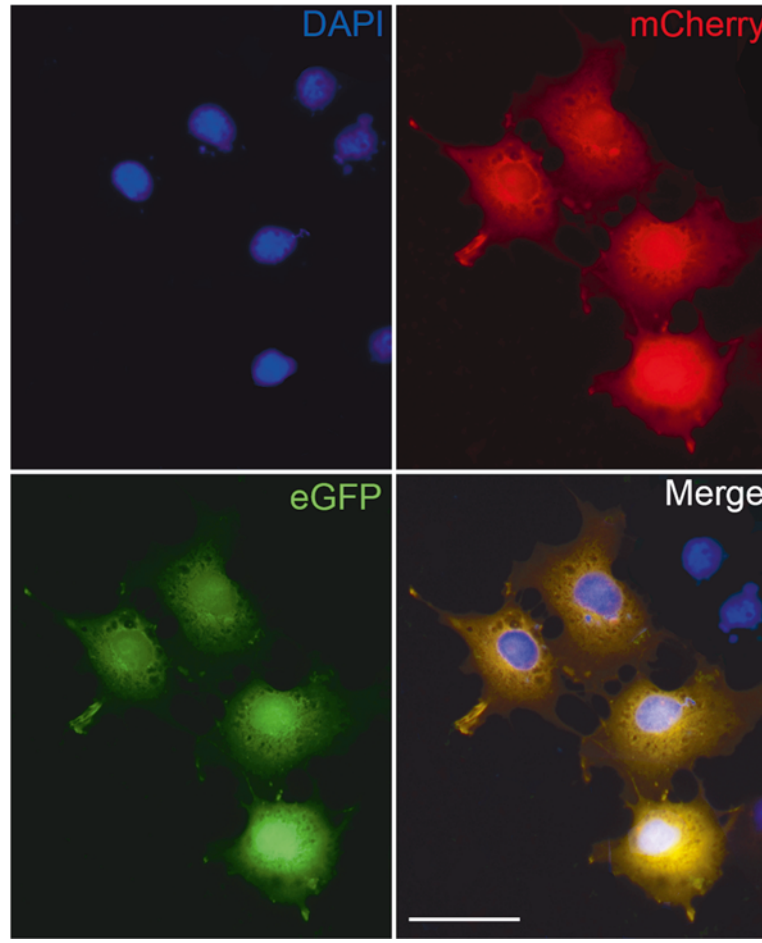

Fig. 2 COS-7 cells transfected with the psub-CMV-mCherry-2A-EGFP-WPRE plasmid efficiently express both mCherry and EGFP. Fluorescent images demonstrate that transfected cells express both mCherry and EGFP and appear *yellow*. Non-transfected cells do not express mCherry or EGFP but can be identified by DAPI staining. Scale bar—25 μm

(because mCherry is in place of a given RAG). It also enabled us to check easily that, indeed, both genes are expressed (Figs. 2 and 3), *see* **Note 2**. Subsequently, we have cloned more than ten different pro-regenerative transgenes in place of mCherry.

Forward and reverse primers were designed for EGFP (Fig. 4) and mCherry (Fig. 5) to ensure that the coding region of the plasmid produced one single open reading frame encoding all of the following: a start codon, the upstream cDNA (mCherry in this case), the 2A sequence, and the downstream cDNA (EGFP in this case), and a stop codon.

For cloning EGFP downstream of the 2A sequence, the forward primer was designed to contain a hexamer of GC repeats (blue) for stability of the PCR product and efficient restriction enzyme cleavage, an MluI restriction site (yellow), and the first

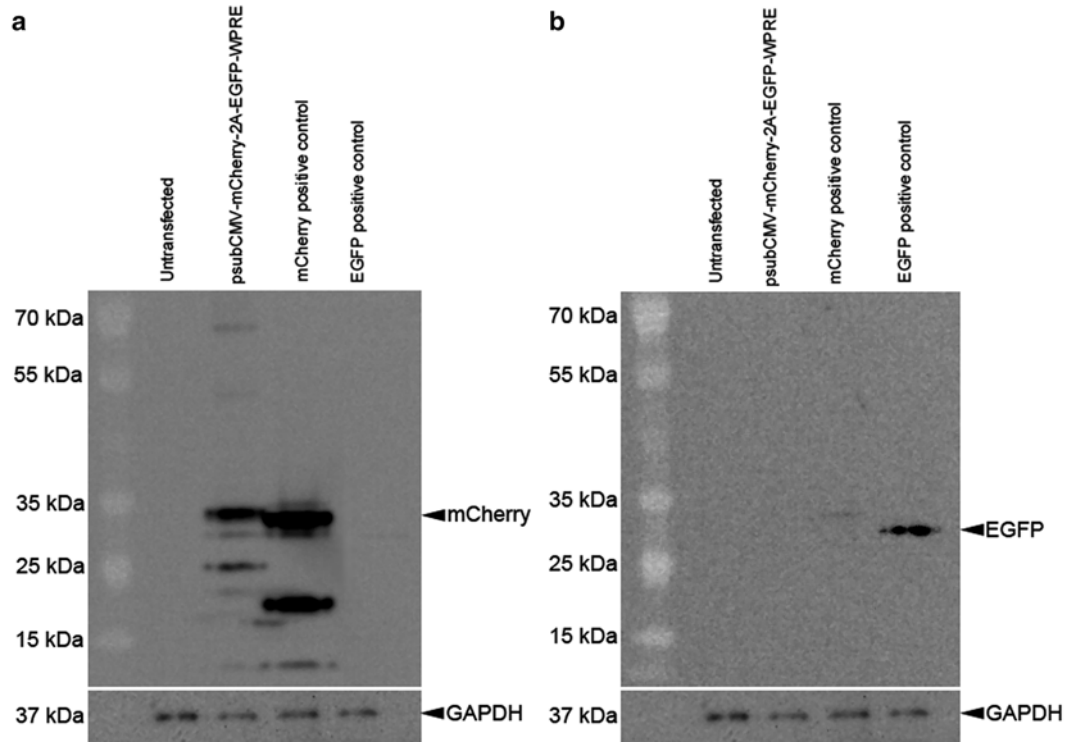

Fig. 3 Western blotting confirms efficient "self-cleavage" of the 2A sequence. COS-7 cells were transfected with the psub-CMV-mCherry-2A-EGFP-WPRE plasmid or the mCherry- or the EGFP-monocistronic plasmids. (**a**) Western blotting of 10 μg of protein lysate using an anti-mCherry antibody (Abcam—ab167453) detected a band at the expected size for mCherry protein (~30 kDa) and was a similar size as our mCherry-positive control (mCherry expressed from a monocistronic plasmid). The mCherry protein from the 2A plasmid was at a slightly larger molecular weight than the control mCherry protein which was expected due to the addition of 23 amino acids at its C-terminus following "self-cleavage" of the 2A sequence. Only a very faint band was detected at ~60 kDa, as would occur if an mCherry-2A-EGFP fusion protein was produced, demonstrating efficient 2A "self-cleavage" of the two proteins. Several unidentified bands were detected at smaller molecular weights for both the 2A plasmid and the mCherry-positive control. (**b**) We were unable to detect EGFP protein expression from the 2A plasmid via western blotting using several different anti-EGFP antibodies (Lifespan Bioscience—C183899, Clontech—632569, Abcam—ab13970, Sigma—G1546). However we did detect a band at the correct size for EGFP (~30 kDa) in our EGFP-positive control (EGFP expressed from a monocistronic plasmid)

28 bases of the EGFP cDNA excluding the ATG start codon, *see* **Note 3**. The reverse primer contained a hexamer of GC repeats (blue), an MluI restriction site (yellow), and the reverse complement of the last 28 bases of the EGFP cDNA (green) including the stop codon (bold and underlined) to ensure that translation ends after the synthesis of the bicistron.

For cloning mCherry upstream of the 2A, the forward primer was designed to contain a hexamer of GC repeats (blue) for stability of the PCR product and efficient restriction enzyme cleavage, a NheI restriction site (pink), and the first 28 bases of the mCherry

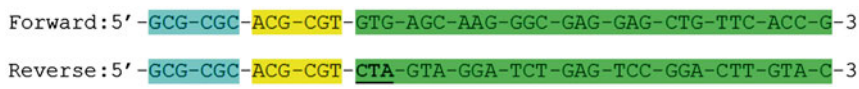

Fig. 4 Primers used for cloning EGFP downstream of 2A

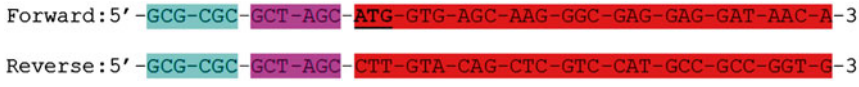

Fig. 5 Primers used for cloning mCherry upstream of 2A

cDNA (red) including the start codon (ATG; bold and underlined). The reverse primer contained the GC repeat hexamer (blue), a NheI restriction site (pink), and the reverse complement of the last 28 bases of the mCherry cDNA with the stop codon excluded (red).

Primers were synthesized at 50 nmol with desalting but no other purification (Sigma, UK). We always check the resulting AAV plasmids by DNA sequencing to ensure that sequences are correct.

Sequencing primer used to check the success of cloning a gene upstream of 2A:

5′-AGC-TGC-GGA-ATT-GTA-CCC-GC-3′

Sequencing primer used to check the success of cloning a gene downstream of 2A:

5′-AAG-GCA-TTA-AAG-CAG-CGT-ATC-CAC-A-3′

2.3 Polymerase Chain Reaction Reagents

The reagents included in our standard PCR were as follows:

	Volume (μL)	Final concentration
DNA template	1	Determined by the user; we used 50 ng
Forward primer (100 μM)	1	1 μM
Reverse primer (100 μM)	1	1 μM
ThermoPol Reaction Buffer (10×)	10	1×
Vent polymerase (2 units/μL)	1	2 units
dNTPs (pool of 10 mM of each)	2	200 μM
DMSO	5	5 %
$MgSO_4$ (100 mM)	4	4 mM
Nuclease-free water	To a final volume of 100 μL	

2.4 Viral Vector Production and Titering

AAV vectors were generated by the Miami Project Viral Vector Core using fast protein liquid chromatography (FPLC)-based purification and pseudotyped with AAV capsid serotype 1, *see* **Note 4**. AAV vectors were suspended in HBSS at 2.9×10^{13} GC/mL, *see* **Note 5**.

2.5 Animals and Surgery

Animals: Female Lister hooded rats weighing 200–220 g (Charles River, UK) were used for these experiments. Rats were maintained under standard animal care conditions (12:12-h light/dark cycle), with food and water ad libitum. All procedures were carried out in accordance with the UK Animals (Scientific Procedures) Act 1986 and approved by the local veterinarian and ethical committee.

Brain atlas for stereotaxic coordinates: Holes were drilled through the skull above the sensorimotor cortex using coordinates reported in a microstimulation mapping study relative to bregma, midline, and the brain surface [36, 37] (*see* Subheading 3 for coordinates).

Stereotaxic apparatus: Stereotaxic frame for rats (World Precision Instruments, FL, USA) which allowed the attachment of a microdrill (Power Performance, UK) or ultra microsyringe pump with Micro4 control panel (World Precision Instruments, FL, USA).

Surgery materials: Eye lubricant (Viscotears, Germany), alcohol-based permanent marker, chlorhexidine disinfectant, sterile cotton buds, small bulldog clamps (World Precision Instruments # 14118), blunted scissors (Fine Science Tools, Fine Scissors—Tough Cut 14058-09), toothed forceps (Fine Science Tools, 11019-12), Long-toothed Alm retractors (Fine Science Tools, 17009-07), fine Dumont forceps (Fine Science Tools, 11251-10), dental hand drill, 0.7 mm drill bits (Fine Science Tools, 19007-07), Vannas Spring Scissors (Fine Science Tools, 15000-03), gelfoam (Equimedical, Gelatin Absorbable Haemostatic Sterile EQU705001), 3.0 Vicryl sutures (Ethicon), scalpel and #10 scalpel blades, needle holder, 27-G needles, 1 mL disposable syringes (for intraperitoneal (i.p.) injection of the anaesthetic), 10 μL Hamilton syringe (Hamilton, Reno, NV, USA), 15 mm, 34 gauge, point style 2, small hub removable needles (Hamilton, 207434), low-magnification stereomicroscope (2–20×).

2.6 Histology, and Microscopy

Fixative and buffers: 4 % paraformaldehyde in phosphate-buffered saline (PBS) pH 7 and cryoprotectant (30 % sucrose in PBS).

Embedding and sectioning: 10 % porcine gelatine in ddH_2O or cryoprotectant embedding medium OCT. A freezing microtome (Leitz, Wetzlar, Germany) or cryostat (Bright, UK) was used to cut the tissue.

Microscope: Confocal microscope (Carl Zeiss LSM 710).

3 Methods

3.1 Plasmid Design and Cloning

1. The coding sequences for mCherry and EGFP were amplified separately using primers and PCR reagents listed above at the cycling conditions recommended by the manufacturer for the Vent polymerase. The conditions for our typical PCR are shown below, *see* **Note 6**:

		Temperature (°C)	Time
1 cycle	Holding	95	2 min
25 cycles	Denaturation	95	30 s
	Annealing	54	30 s
	Extension	73	3 min
1 cycle	Final extension	73	11 min

2. An aliquot of the amplicons (2.5 μL of the 100 μL reaction) was analyzed using agarose gel electrophoresis to ensure that the PCR products were of the expected sizes.
3. These blunt-ended amplicons were separately cloned into the pCR-BluntII-TOPO plasmid (Invitrogen, UK) according to the manufacturer's instructions, creating pCR-BluntII-TOPO-mCherry and pCR-BluntII-TOPO-EGFP. Competent *E. coli* were then transformed using the heat-shock protocol and 3 μL of the cloning reaction. Transformants were streaked out onto LB-agar plates containing kanamycin (10 μg/mL).
4. A day later, putative positive clones were inoculated into 5 mL of LB-kanamycin and DNA was purified using standard mini-preps (Promega, UK).
5. Clones were screened by restriction digests of the purified DNA using 0.5–1.0 μg of pCR-BluntII-TOPO-mCherry or pCR-BluntII-TOPO-EGFP digested by NheI or MluI, respectively. Our standard screening restriction digests were as follows, *see* **Note 7**:

Reagent	Volume
DNA (up to 1 μg)	1 μL
10× Buffer 4	2 μL
100× BSA	0.2 μL
Restriction enzyme (NheI or MluI)	0.5 μL (2–10 units)
Nuclease-free water	To a final volume of 20 μL

6. Clones were screened by performing an MluI or an NheI restriction digest and visualized using agarose gel electrophoresis to ensure that the cDNA inserts were present. Subsequently,

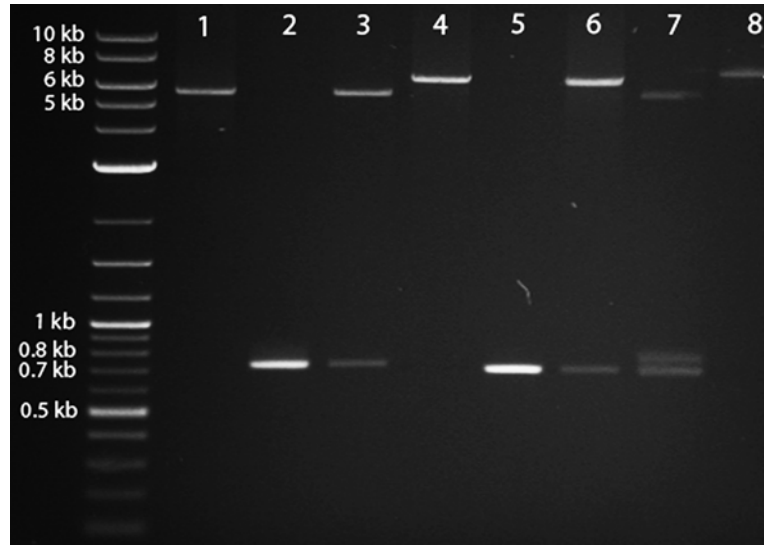

Fig. 6 Agarose gel electrophoresis of restriction-digested plasmid DNA depicts the expected products at each step when cloning mCherry and EGFP into the psub-CMV-2A-WPRE plasmid. See text for a detailed explanation of the steps illustrated in the figure

these clones were sequenced using the SP6 and T7 primer sites that flank the "multiple cloning site" of pCR-Blunt II-TOPO to ensure the fidelity of the PCR amplification.

7. At least 10 μg of the psub-CMV-2A-WPRE vector was digested with MluI and then treated with alkaline phosphatase to prevent re-circularization. Similarly, 10 μg of pCR-BluntII-TOPO-EGFP was also digested with MluI to release the EGFP cDNA. Both the vector (Fig. 6, lane 1) and the insert (Fig. 6, lane 2) were then purified using gel extraction.
8. The EGFP cDNA insert was then ligated into the vector using T4 DNA ligase, following the manufacturer's protocol, to create psub-CMV-2A-EGFP-WPRE.
9. This new plasmid was transformed into *E. coli*, and clones were screened for the presence of the insert using an MluI restriction digest (as described above) (Fig. 6, lane 3) and then sequenced to ensure the correct orientation of the EGFP insert.
10. Next, to clone in mCherry upstream of the 2A-EGFP sequence, psub-CMV-2A-EGFP-WPRE was digested with NheI and treated with alkaline phosphatase. The pCR-BluntII-TOPO-mCherry was also digested with NheI to release the mCherry cDNA.

11. The linearized psub-CMV-2A-EGFP-WPRE (Fig. 6, lane 4) and the mCherry cDNA insert (Fig. 6, lane 5) were gel purified and then ligated using T4 DNA ligase to create psub-CMV-mCherry-2A-EGFP-WPRE and transformed into *E. coli*. The following day, DNA minipreps were obtained for 10–20 colonies.
12. Clones were screened for the presence of the insert via NheI restriction digest (Fig. 6, lane 6) and then sequenced to ensure the correct orientation of mCherry.
13. psub-CMV-mCherry-2A-EGFP-WPRE was digested with MluI and NheI to show the presence of both EGFP and mCherry (Fig. 6, lane 7).
14. psub-CMV-mCherry-2A-EGFP-WPRE was digested with XhoI to illustrate the increased size of the linearized plasmid (Fig. 6, lane 8) relative to lanes 1 and 4.

3.2 Electroporation of Plasmids

1. Because it is expensive to generate AAV vectors, we routinely screen newly cloned AAV transfer plasmids in vitro using electroporation [38]. We can check that the plasmid is expressing the reporter protein (Fig. 2), and, if the plasmid contains a RAG, that it promotes neurite outgrowth, *see* **Note 8**.

3.3 Viral Vector Production and Titering

1. AAV vectors were generated by the Miami Project Viral Vector Core using FPLC-based purification.
2. The AAV vector transgene cassette was flanked by noncoding inverted terminal repeats (ITRs), which were the only wild-type viral sequences present. The AAV vectors were pseudotyped with AAV capsid serotype 1. Following production, the AAV vectors were titered using quantitative PCR to determine the number of genomic copies and an infection assay on 293 T cells was conducted to verify transduction efficiency.

3.4 Intracortical Injections

1. Female adult Lister hooded rats (Charles River, UK) weighing 200–220 g were anesthetized with an intraperitoneal injection of 0.5 mg/kg Domitor (medetomidine hydrochloride) and 100 mg/kg Vetalar (ketamine hydrochloride).
2. Once anesthetized, the head was shaved and sterilized using chlorhexidine disinfectant.
3. Eye lubricant was applied to the eyes, and throughout the surgery, the animals' body temperature was maintained at 37 °C with a thermal heating blanket connected to a rectal temperature probe.
4. The rats' head was placed into the stereotaxic frame, and the incisor bar was lowered 2 mm below the horizontal plane so

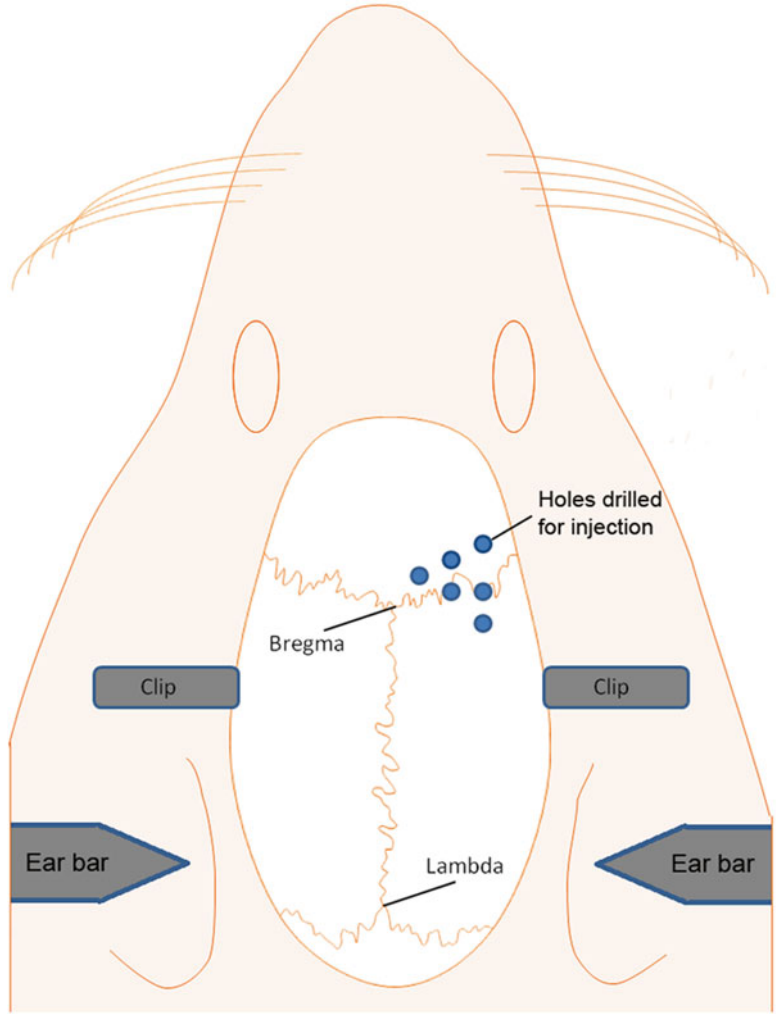

Fig. 7 Schematic showing the position of the holes drilled into the skull, relative to bregma, to expose the sensorimotor cortex for AAV vector injection. See text for a detailed explanation of the drilling and injection procedure

that the heights of lambda and bregma were equal and the surface of the skull was flat (Fig. 7).

5. Following a midline incision, the skin was retracted using small bulldog clamps and the periosteum was removed with a scalpel blade to expose the skull surface.
6. The microdrill was fixed to the stereotaxic frame holder and the drill burr centred over bregma. Six holes were then drilled through the skull above the left or the right sensorimotor cortex using coordinates reported in a microstimulation mapping study relative to bregma, midline, and the brain surface (Fig. 7). Defined as anterior–posterior (AP), medial–lateral (ML), and dorsal–ventral (DV):

First: 3.5 mm ML, –0.5 mm AP, DV –1.5 mm.

Second: 3.5 mm ML, +0.5 mm AP, DV –1.5 mm.

Third: 3.5 mm ML, +2 mm AP, DV –1.5 mm.

Fourth: 2.5 mm ML, +1.5 mm AP, DV –1.5 mm.

Fifth: 2.5 mm ML, +0.5 mm AP, DV –1.5 mm.

Sixth: 1.5 mm ML, +1 mm AP, DV –1.5 mm.

7. A 10 μL Hamilton syringe fitted with a 15 mm, 34 gauge, small hub removable needle was loaded with 3 μL of viral vector and fixed to the stereotaxic frame holder.
8. The tip of the needle was positioned over the first hole and lowered onto the brain surface. Once on the brain surface it was lowered a further 1.5 mm into the sensorimotor cortex.
9. 0.5 μL of AAV vector was infused into the brain using a microsyringe pump. The infusion rate was set to 200 nL/min on the Micro4 control panel, *see* **Note 9**.
10. Once the pump infusion was finished the needle was left in place for 3 min to allow the AAV vector to diffuse from the injection site.
11. The needle was then removed and positioned at the second coordinate to inject the next 0.5 μL of AAV vector. This process was repeated until all six injections were complete.
12. After the last injection the skin was closed using 3.0 vicryl sutures.
13. The rats were then placed into an incubator at 37 °C and 1 mg/kg Antisedan (atipamezole hydrochloride) was administered Subcutaneously. Once awake, 5 mg/kg Carprofen was administered subcutaneously for postoperative analgesia.

3.5 Pyramidotomy Injury Model

1. Rats were anesthetized using 5 % isoflurane in O_2 (flow rate 1.5 L/min) and maintained with 1–2 % isoflurane in O_2. Throughout the surgery the animals' body temperature was maintained at 37 °C with a thermal heating blanket connected to a rectal temperature probe, *see* **Note 10**.
2. The ventral neck region was shaved and sterilized using chlorhexidine disinfectant.
3. A midline incision is made from the chin to the rostral end of the sternum and the outer layers of gland, and muscle tissue is blunt dissected until the trachea is exposed.
4. The trachea is displaced slightly to one side, and the underlying muscle is dissected rostrally until the basioccipital skull is reached, *see* **Note 11**.
5. Surgical long-teethed retractors are inserted to allow access to the basioccipital bone.

6. A craniotomy of the ventral occipital bone was performed using a microdrill. This allows access to the medullary pyramids, which are located medially.
7. The left or the right pyramid was cut using Vannas microscissors making sure that the medial boundary close to the basilar artery is lesioned as well, *see* **Notes 12–14**.
8. Any bleeding is stopped, and the skin is sutured using 3.0 vicryl sutures.
9. The rats were placed in an incubator at 37 °C until fully awake. 5 mg/kg Carprofen was administered subcutaneously for postoperative analgesia.

3.6 Histology

1. 10 weeks post-injection, the rats were terminally anesthetized by intraperitoneal injection of 400 mg/kg Euthasol (sodium pentobarbital) and transcardially perfused with 200 mL PBS (pH 7.4) to remove the blood, followed by 200 mL 4 % paraformaldehyde in PBS (pH 7.4).
2. Immediately following perfusion the brain and spinal cord were dissected and post-fixed in 4 % paraformaldehyde in PBS for 2 h at 4 °C.
3. The tissue was then cryoprotected in 30 % sucrose with 0.1 % sodium azide for 5 days at 4 °C.
4. The brain and spinal cord tissue were placed in small plastic boxes and blocked in porcine gelatin.
5. Once the gelatin had set, they were placed overnight in 4 % paraformaldehyde in PBS at 4 °C to harden.
6. To allow tissue from each brain to undergo different immunohistological analysis the brains were cut rostro-caudally into 50 μm coronal serial sections using a freezing microtome and collected into ten series in a 24-well plate containing PBS and 0.1 % sodium azide. The spinal cords were cut rostro-caudally into 30 μm transverse serial sections and stored in the same manner.
7. The tissue sections were then mounted onto microscope slides using Mowiol and kept in the dark.

3.7 Microscopy

1. Slides were imaged using a confocal microscope (Fig. 8).

4 Notes

1. The cloning capacity of AAVs is approximately 5 kB from ITR to ITR, and longer sequences may lead to poor packaging and reduced titers. When using psubCMV-2A-EGFP-WPRE, only about 2.1 kb is available for a transgene. However, if longer

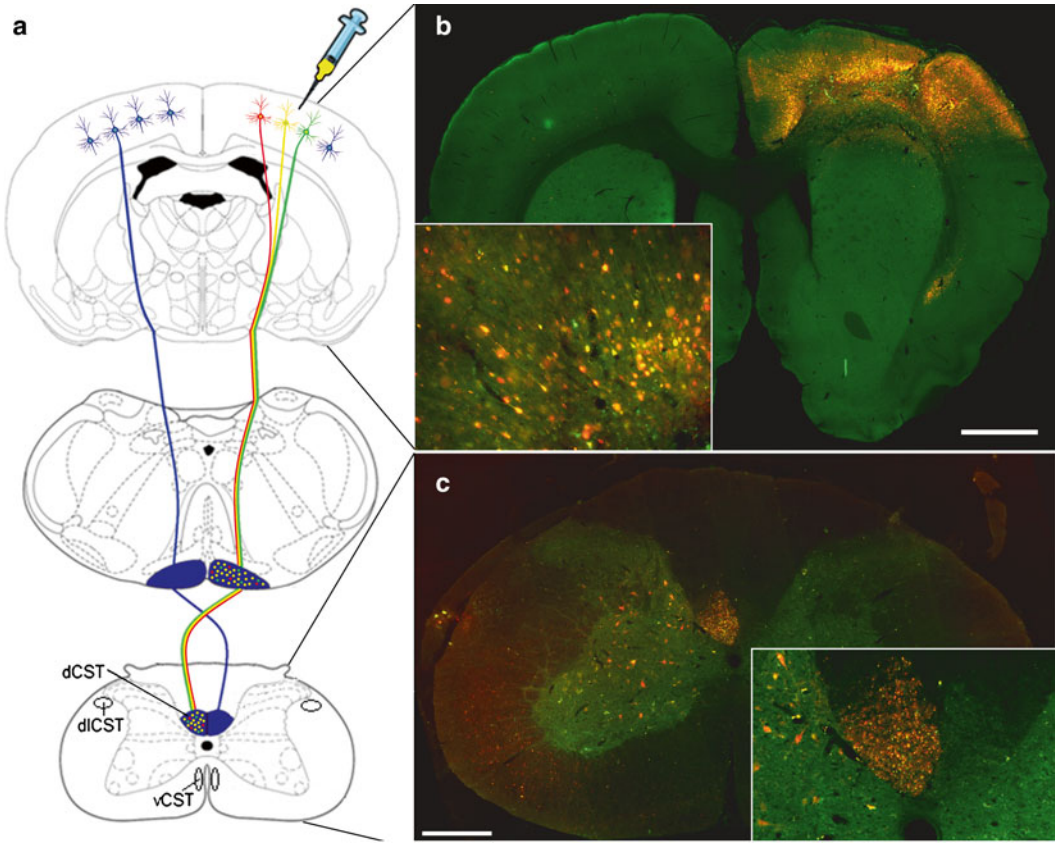

Fig. 8 (**a**) Schematic representation showing the rodent CST originating from the pyramidal CSNs in layer V of the sensorimotor cortex, decussating at the spinomedullary junction, forming the main dCST and the minor dlCST and vCST. (**b**) Image showing widespread transduction of the cortex; many cortical neurons including CSNs in layer V are expressing both mCherry and EGFP (cells appear *yellow*). (**c**) Image showing numerous mCherry- and EGFP-positive CST axons (axons appear *yellow*) in the contralateral dCST of the cervical spinal cord. Unexpectedly, some fibers in the dorsal columns appear to be just mCherry or EGFP positive. We are unsure why this is, but it may reflect differences in the vesicular transport of the two proteins. Others have reported similar issues (Wall et al [39] and references therein). Moreover, we have not yet been able to detect transgene positive axon collaterals in the spinal grey matter

transgenes need to be expressed, then WPRE could be deleted to make additional space.

2. EGFP protein could not be detected from the 2A plasmids via western blotting. This is a highly surprising result considering that the transfected COS-7 cells strongly expressed EGFP (Fig. 3) and our EGFP-positive control (EGFP expressed from a monocistronic plasmid) worked. Possible explanations for this may be because part of the "self-cleaved" 2A sequence remains attached to the N-terminus of EGFP and prevents binding to the anti-EGFP antibodies. However this is unlikely as we have tested several different antibodies (Lifespan Bioscience—C183899, Clontech—632569, Abcam—ab13970,

Sigma—G1546) raised against different regions of the EGFP protein including the N- and C-terminus, and the C-terminus of the downstream gene should not be affected by "self-cleavage" of the 2A sequence.

3. Note that our intermediate plasmid (psub-CMV-2A-EGFP) will not express EGFP in vitro or in vivo unless a transgene (containing an appropriate start codon) is cloned upstream of 2A.
4. It is important to choose the correct AAV serotype for the cell type you wish to transduce. We and others have previously shown that AAV1 and 5 are the optimal serotypes for transducing cortical neurons.
5. Using high-titer AAV vectors is a crucial factor for achieving high-level transduction, ideally 1×10^{13} GC/mL or higher.
6. The extension time of the PCR cycle was increased in instances where the cDNA was significantly larger. Some of the RAGs we cloned were over 3,000 bp long and required an increase in the extension time to 6 min.
7. The cDNA to be inserted must be checked to ensure that none of the restriction sites used for cloning (MluI and NheI) are present within the coding region. For example one of our RAGs contained an NheI site within its coding sequence. We replaced the NheI restriction site of the upstream and downstream primers with an SpeI restriction site that has an identical overhang to NheI. However, a ligation of DNA products digested by NheI and SpeI loses the restriction site for both enzymes and it cannot be subsequently restriction digested by either enzyme.
8. Note that "self-cleavage" of the 2A plasmid results in the upstream gene product having an additional 23 amino acids attached to the C-terminus and the downstream gene product having one additional amino acid attached to the N-terminus (Fig. 1b). The consequences of this additional sequence need to be verified empirically on a case-by-case basis, but in our experience, most pro-regenerative genes continue to show pro-regenerative effects in vitro after being shuttled from a monocistronic plasmid into the bicistronic psub-CMV-2A-EGFP-WPRE plasmid.
9. An important step in achieving high levels of transduction and a large area of transduction is the use of a micropump to slowly inject the viral vector over several minutes. In addition once the injection is complete it is also important to leave the needle in place for at least a couple of minutes to allow viral vector diffusion away from the injection sites.
10. The pyramidotomy surgery requires practice. High mortality rates are associated with the pyramidotomy surgery (*see* Steward et al. [40] and Kathe et al. [41]).
11. Displacement of the trachea can cause breathing difficulties or apnea. Giving Dopram (Dopram V-Drops, 20 mg/mL),

a respiratory stimulant, during the surgery can increase breathing activity. Furthermore, loosening of the retractors multiple times during the surgery can stabilize the animal.

12. When the pyramids are lesioned the basilar artery should be avoided. In addition to this, if the cut is made too deep it can affect the midbrain nuclei that are part of the breathing and cardiovascular centers.
13. Lesions are often incomplete. Repeating the cut with a 26 G needle including the fibers close to the basilar artery will prevent this to some extent.
14. Immunohistochemical staining for PKCγ can be used to verify completeness of the pyramidotomy lesion.

Acknowledgments

We would like to thank Dr. Vance Lemmon and the Miami Vector Core for production of the AAV vectors. We would also like to acknowledge support from a Research Councils UK Academic Fellowship (L.M.), the British Pharmacological Society's Integrative Pharmacology Fund (L.M), Friends of Guy's Hospital Research Grants (L.M.), and a grant from the Henry Smith Charity (L.M. and T.H.).

References

1. Chen DF, Jhaveri S, Schneider GE (1995) Intrinsic changes in developing retinal neurons result in regenerative failure of their axons. Proc Natl Acad Sci U S A 92:7287–7291
2. Nicholls JG, Saunders N (1996) Regeneration of immature mammalian spinal cord after injury. Trends Neurosci 19:229–234
3. Goldberg JL (2004) Intrinsic neuronal regulation of axon and dendrite growth. Curr Opin Neurobiol 14:551–557
4. Goldberg JL, Klassen MP, Hua Y et al (2002) Amacrine-signaled loss of intrinsic axon growth ability by retinal ganglion cells. Science 296: 1860–1864
5. Afshari FT, Kappagantula S, Fawcett JW (2009) Extrinsic and intrinsic factors controlling axonal regeneration after spinal cord injury. Expert Rev Mol Med 11:e37
6. Blackmore MG, Wang Z, Lerch JK et al (2012) Kruppel-like Factor 7 engineered for transcriptional activation promotes axon regeneration in the adult corticospinal tract. Proc Natl Acad Sci U S A 109:7517–7522
7. Yip PK, Wong LF, Pattinson D et al (2006) Lentiviral vector expressing retinoic acid receptor {beta}2 promotes recovery of function after corticospinal tract injury in the adult rat spinal cord. Hum Mol Genet 15:3107–3118
8. Yip PK, Wong LF, Sears TA et al (2010) Cortical overexpression of neuronal calcium sensor-1 induces functional plasticity in spinal cord following unilateral pyramidal tract injury in rat. PLoS Biol 8:e1000399
9. Moore DL, Blackmore MG, Hu Y et al (2009) KLF family members regulate intrinsic axon regeneration ability. Science 326:298–301
10. Tracey DJ (1995) Ascending and descending pathways in the spinal cord. The rat nervous system, 2nd edn. Academic, San Diego, CA, pp 67–77
11. Lemon RN (2008) Descending pathways in motor control. Annu Rev Neurosci 31: 195–218
12. Whishaw IQ, Gorny B, Sarna J (1998) Paw and limb use in skilled and spontaneous reaching after pyramidal tract, red nucleus and combined lesions in the rat: behavioral and

anatomical dissociations. Behav Brain Res 93: 167–183

13. Whishaw IQ, Metz GA (2002) Absence of impairments or recovery mediated by the uncrossed pyramidal tract in the rat versus enduring deficits produced by the crossed pyramidal tract. Behav Brain Res 134: 323–336
14. Starkey ML, Barritt AW, Yip PK et al (2005) Assessing behavioural function following a pyramidotomy lesion of the corticospinal tract in adult mice. Exp Neurol 195:524–539
15. Thallmair M, Metz GAS, Z'Graggen WJ et al (1998) Neurite growth inhibitors restrict plasticity and functional recovery following corticospinal tract lesions. Nat Neurosci 1: 124–131
16. Cafferty WB, Strittmatter SM (2006) The Nogo-Nogo receptor pathway limits a spectrum of adult CNS axonal growth. J Neurosci 26:12242–12250
17. Hutson TH, Verhaagen J, Yanez-Munoz RJ et al (2012) Corticospinal tract transduction: a comparison of seven adeno-associated viral vector serotypes and a non-integrating lentiviral vector. Gene Ther 19:49–60
18. McCown TJ (2005) Adeno-associated virus (AAV) vectors in the CNS. Curr Gene Ther 5:333–338
19. Papale A, Cerovic M, Brambilla R (2009) Viral vector approaches to modify gene expression in the brain. J Neurosci Methods 185:1–14
20. Kaplitt MG, Feigin A, Tang C et al (2007) Safety and tolerability of gene therapy with an adeno-associated virus (AAV) borne GAD gene for Parkinson's disease: an open label, phase I trial. Lancet 369:2097–2105
21. Lim ST, Airavaara M, Harvey BK (2009) Viral vectors for neurotrophic factor delivery: a gene therapy approach for neurodegenerative diseases of the CNS. Pharmacol Res 61:14–26
22. Yla-Herttuala S (2012) Endgame: glybera finally recommended for approval as the first gene therapy drug in the European union. Mol Ther 20:1831–1832
23. Vandenberghe LH, Wilson JM, Gao G (2009) Tailoring the AAV vector capsid for gene therapy. Gene Ther 16:311–319
24. Burger C, Nash K, Mandel RJ (2005) Recombinant adeno-associated viral vectors in the nervous system. Hum Gene Ther 16: 781–791
25. Cearley CN, Wolfe JH (2006) Transduction characteristics of adeno-associated virus vectors expressing cap serotypes 7, 8, 9, and Rh10 in the mouse brain. Mol Ther 13:528–537
26. Rabinowitz JE, Rolling F, Li C et al (2002) Cross-packaging of a single adeno-associated virus (AAV) type 2 vector genome into multiple AAV serotypes enables transduction with broad specificity. J Virol 76:791–801
27. Foust KD, Flotte TR, Reier PJ et al (2008) Recombinant adeno-associated virus-mediated global anterograde delivery of glial cell line-derived neurotrophic factor to the spinal cord: comparison of rubrospinal and corticospinal tracts in the rat. Hum Gene Ther 19:71–82
28. Blits B, Derks S, Twisk J et al (2010) Adeno-associated viral vector (AAV)-mediated gene transfer in the red nucleus of the adult rat brain: comparative analysis of the transduction properties of seven AAV serotypes and lentiviral vectors. J Neurosci Methods 185:257–263
29. Burger C, Gorbatyuk OS, Velardo MJ et al (2004) Recombinant AAV viral vectors pseudotyped with viral capsids from serotypes 1, 2, and 5 display differential efficiency and cell tropism after delivery to different regions of the central nervous system. Mol Ther 10:302–317
30. Taymans JM, Vandenberghe LH, Haute CV et al (2007) Comparative analysis of adeno-associated viral vector serotypes 1, 2, 5, 7, and 8 in mouse brain. Hum Gene Ther 18: 195–206
31. Klein RL, Lewis MH, Muzyczka N et al (1999) Prevention of 6-hydroxydopamine-induced rotational behavior by BDNF somatic gene transfer. Brain Res 847:314–320
32. Martinez-Salas E (1999) Internal ribosome entry site biology and its use in expression vectors. Curr Opin Biotechnol 10:458–464
33. Mizuguchi H, Xu Z, Ishii-Watabe A et al (2000) IRES-dependent second gene expression is significantly lower than cap-dependent first gene expression in a bicistronic vector. Mol Ther 1:376–382
34. Furler S, Paterna JC, Weibel M et al (2001) Recombinant AAV vectors containing the foot and mouth disease virus 2A sequence confer efficient bicistronic gene expression in cultured cells and rat substantia nigra neurons. Gene Ther 8:864–873
35. Minskaia E, Nicholson J, Ryan MD (2013) Optimisation of the foot-and-mouth disease virus 2A co-expression system for biomedical applications. BMC Biotechnol 13:67
36. Paxinos G, Watson C (1982) The rat brain in stereotaxic coordinates. Academic, San Diego, CA
37. Neafsey EJ, Bold EL, Haas G et al (1986) The organization of the rat motor cortex: a microstimulation mapping study. Brain Res 396: 77–96

38. Hutson TH, Buchser WJ, Bixby JL et al (2011) Optimization of a 96-well electroporation assay for postnatal rat CNS neurons suitable for cost-effective medium-throughput screening of genes that promote neurite outgrowth. Front Mol Neurosci 4:55
39. Wall NR, Wickersham IR, Cetin A et al (2010) Monosynaptic circuit tracing in vivo through Cre-dependent targeting and complementation of modified rabies virus. PNAS 107:21848–21853
40. Steward O, Sharp K, Yee KM (2012) A re-assessment of the effects of intracortical delivery of inosine on transmidline growth of corticospinal tract axons after unilateral lesions of the medullary pyramid. Exp Neurol 233: 662–673
41. Kathe C, Hutson TH, Chen Q, Shine HD, McMahon SB, Moon, LDF, Unilateral pyramidotomy of the corticospinal tract in rats for assessment of neuroplasticity inducing therapies. Accepted for publication in JoVe